Kinetic Study of N-Type Calcium Current Modulation by δ-Opioid Receptor Activation in the Mammalian Cell Line NG108-15

Mauro Toselli, Patrizia Tosetti, and Vanni Taglietti
Istituto di Fisiologia Generale, Universita' di Pavia and Istituto Nazionale per la Fisica della Materia, Pavia Unit, I-27100 Pavia, Italy

ABSTRACT The voltage-dependent inhibition of N-type Ca^{2+} channel current by the δ-opioid agonist [D-pen^2, D-pen^5]-enkephalin (DPDPE) was investigated in the mammalian cell line NG108-15 with 10 μM nifedipine to block L-type channels, with whole-cell voltage clamp methods. In in vitro differentiated NG108-15 cells DPDPE reversibly decreased ω-conotoxin GVIA-sensitive Ba^{2+} currents in a concentration-dependent way. Inhibition was maximal with 1 μM DPDPE (66% at 0 mV) and was characterized by a slowing of Ba^{2+} current activation at low test potentials. Both inhibition and kinetic slowing were attenuated at more positive potentials and could be relieved up to 90% by strong conditioning depolarizations. The kinetics of removal of inhibition (de-inhibition) and of its retrieval (re-inhibition) were also voltage dependent. Both de-inhibition and re-inhibition were single exponentials and, in the voltage range from −20 to +10 mV, had significantly different time constants at a given membrane potential, the time course of re-inhibition being faster than that of de-inhibition. The kinetics of de-inhibition at −20 mV and of reinhibition at −40 mV were also concentration dependent, both processes becoming slower at lower agonist concentrations. The rate of de-inhibition at +80/+120 mV was similar to that of Ca^{2+} channel activation at the same potentials measured during application of DPDPE (~7 ms), both processes being much slower than channel activation in controls (<1 ms). Moreover, the amplitude but not the time course of tail currents changed as the depolarization to +80/+120 mV was made longer. The state-dependent properties of DPDPE Ca^{2+} channel inhibition could be simulated by a model that assumes that inhibition by DPDPE results from voltage- and concentration-dependent binding of an inhibitory molecule to the N-type channel.

INTRODUCTION

Many kinds of transmitters, hormones, and peptides inhibit neuronal voltage-dependent Ca^{2+} channels by activation of specific plasma membrane receptors (for a review see Carbone and Swandulla, 1989). In most cases the modulatory pathway is membrane delimited, where an activated inhibitory macromolecule, possibly a pertussis-toxin-sensitive GTP-binding protein, directly interacts with the Ca^{2+} channel (Lopez and Brown, 1991; Boland and Bean, 1993, Qin et al., 1997; Zamponi and Snutch, 1998).

Ca^{2+} channel current inhibition is often coupled to changes in current kinetics and voltage dependence. Current is inhibited more at small depolarizations than at large depolarizations, and modulators induce a slow phase of activation (Bean, 1989; Grassi and Lux, 1989; Elmslie et al., 1990; Lopez and Brown, 1991; Pollo et al., 1992; Kasai, 1992; Golard and Siegelbaum, 1993; Toselli et al., 1995). In a few cases, voltage- and time-dependent Ca^{2+} channel modulation could also be observed at the single-channel level (Toselli and Taglietti, 1994; Carabelli et al., 1996). Those observations offer some indications as to how inhibition could occur. However, knowledge of the mechanism is fragmentary, and some contradictory results have been reported, for instance, the dependence of inhibition kinetics on the extent of activated G proteins (Lopez and Brown, 1991; Elmslie and Jones, 1994; Toselli et al., 1997; Kasai, 1992; Pollo et al., 1992) or the dependence of tail current amplitude and kinetics on the duration of strongly depolarizing test pulses. (Pollo et al., 1992; Toselli et al., 1995; Boland and Bean, 1993). Those different results suggest different kinetic models of Ca channel modulation.

In the present work, our goal was to study in more detail the mechanisms of N-type Ca^{2+} channel inhibition, to have a rigorous and complete description of channel behavior at different agonist concentrations and in a wide voltage range. In particular the points on which we mainly focused our attention were the following. 1) In addition to their dependence on voltage, are the slow kinetics, after depolarization or repolarization, also concentration dependent? 2) Are current de-inhibition (caused by depolarization) and re-inhibition (caused by repolarization) specular processes following the same kinetics? 3) Do channel de-inhibition and activation proceed at the same or different rates? This information is crucial to propose a comprehensive model of N-type Ca^{2+} channel inhibition and to discover whether facilitation could be physiologically important.

We have studied inhibition of N-type ω-conotoxin fraction (ω-CgTx) GVIA-sensitive Ca^{2+} channel current by the δ-opioid agonist [D-pen^2, D-pen^5]-enkephalin (DPDPE) in NG108-15 cells. The mammalian neuroblastoma-glioma cell line NG108-15 acquires a neuronal phenotype after in vitro differentiation and expresses high-voltage-activated (HVA) ω-CgTx GVIA-sensitive Ca^{2+} channels (Kasai and Neher, 1992) that can be modulated by neurotransmitters and opioids (Tsunoo et al., 1986; Taussig et al., 1992; Kasai,

Received for publication 26 January 1998 and in final form 18 November 1998.

Address reprint requests to Dr. M. Toselli, Istituto di Fisiologia Generale, Via Forlanini 6, I-27100 Pavia, Italy. Tel.: 39-382-507612; Fax: 39-382-507527; E-mail: mtoselli@ipv36.unipv.it.

0006-3495/99/05/2560/15 $2.00

1992). These features make this subclone a highly suitable model for the study of voltage-operated Ca^{2+} channel modulation in neurons.

At least three important observations reported here show that the mechanism underlying N-type Ca^{2+} channel facilitation in NG108-15 cells differs from what has been shown for sympathetic or other neurons.

The most important features of Ca^{2+} channel current inhibition in NG108-15 cells could be simulated by a kinetic model that differs significantly from those proposed by others (Bean, 1989; Elmslie et al., 1990; Lopez and Brown, 1991; Kasai, 1992; Pollo et al., 1992; Boland and Bean, 1993). Moreover, some of our experimental observations and the model suggest some basic criteria to state whether facilitation could be of physiological relevance.

MATERIALS AND METHODS

Cell culture

The cells were grown in monolayers in Dulbecco's modified Eagle's medium (DMEM), 10% heat-inactivated fetal calf serum, hypoxanthine-aminopterin-thymidine (HAT) supplement, 100 μg of streptomycin/ml, and 100 IU of penicillin/ml (Sigma Chemical Co., St. Louis, MO) in a 5% CO_2 humidified atmosphere at 37°C. Cells were plated both in plastic petri dishes (also used for electrophysiological experiments) and in plastic flasks (used for cell subcultivation when confluent). The medium was replaced three times a week. Differentiation of NG108-15 cells was stimulated by culturing the cells (at ~30% confluence) with 10 μM prostaglandin E_1 (ICN Biomedicals, Opera, Italy) and 1 mM theophylline (Sigma Chemical Co.). Cells were treated with the differentiating agents for at least 5 days before use.

Electrophysiology

Whole-cell patch-clamp currents were recorded at room temperature (20–24°C) with a LIST LM/EPC7 patch-clamp amplifier (List Electronic, Darmstadt, Germany) and digitized at sampling intervals of 26–100 μs using a 12-bit A/D Tecmar LabMaster board interfaced with an Olivetti M 380/C PC. Stimulation, acquisition, and data analysis were carried out with pClamp (Axon Instruments, Burlingame, CA) and ORIGIN (Microcal Software, Northampton, MA).

Linear components of leak and capacitive currents were first reduced by analog circuitry and then almost completely canceled with the P/N method. Patch pipettes were made from borosilicate glass tubing (Bardram, Birkerod, Denmark) and fire polished. Pipettes had a final resistance of 0.5–2 MΩ when filled with internal solution.

Experiments were performed on cells with small processes to guarantee sufficient voltage and space clamp control. Cells were discarded if current tracings showed signs of notch-like current discontinuities. Current run-down was relatively slow; on the average we measured a current decrease of less than 10% within 15 min. This allowed the application of more than one protocol in each cell. A sampling interval of 25 μs/point and series resistance compensation of 50–70% were applied when tail currents were studied. Currents were filtered at 3 KHz.

Numerical data in the text are mean values ± SD.

Solutions

The patch pipettes were filled with (in mM) 120 CsCl, 20 tetraethylammonium chloride, 10 EGTA, 2 $MgCl_2$, 4 Mg-ATP, 0.1 GTP, 10 HEPES/CsOH (pH 7.4). Seals between electrodes and cells were established in a solution consisting of (in mM) 135 NaCl, 1.8 $CaCl_2$, 2 $MgCl_2$, 5.5 KCl, 10 glucose, 10 HEPES/NaOH (pH 7.4). After establishing the whole-cell configuration, cells were perfused with an external saline containing (in mM) 130 NaCl, 10 $BaCl_2$, 2 $MgCl_2$, 10 glucose, 10 HEPES/NaOH (pH 7.4), 1,4-aminopyridine, 10 tetraethylammonium chloride, 10^{-3} tetrodotoxin (Sigma Chemical Co.). During recording, extracellular Ca^{2+} was substituted with Ba^{2+} to minimize Ca^{2+}-dependent inactivation of Ca^{2+} channel currents. In most experiments nifedipine (Bayer AG, Wuppertal, Germany) at a final concentration of 10 μM was added to the external saline. External solutions were exchanged by a fast multi-barrel delivery system positioned close to the cell. Changes between control and test solutions were made using electrovalves (Festo S.p.A., Assago, Italy) operated by computer-synchronized commands that allowed a complete replacement of the solution surrounding the cell within ~50 ms. The δ opiate agonist DPDPE was purchased from Sigma Chemical Co., and ω-CgTx GVIA from Peninsula Laboratories (St. Helens, UK).

RESULTS

Most of in vitro differentiated NG108-15 cells express both low-voltage-activated (LVA) and high-voltage-activated (HVA) L-type (nifedipine-sensitive) and N-type (ω-CgTx GVIA-sensitive) Ca^{2+} channels (Tsunoo et al., 1986; Kasai and Neher, 1992). As our main interest in this study was to investigate N-type Ca^{2+} channel modulation, 10 μM nifedipine and −40 mV holding potential were used in all experiments (except where noted) to eliminate contamination from LVA and L-type Ca^{2+} currents when present.

DPDPE inhibits N-type Ca^{2+} channel current

As reported by Kasai (1992), DPDPE inhibited a large fraction of the ω-CgTx GVIA-sensitive Ba^{2+} current in NG108-15 differentiated cells (Fig. 1, upper tracings). The inhibition by DPDPE was reliable (present in 228 cells of 251 tested), completely reversible, and large, the agonist inhibiting 66 ± 6% of the ω-CgTx GVIA-sensitive current at saturating concentrations of 0.1–1 μM ($n = 59$).

The effect of DPDPE on the ω-CgTx GVIA-sensitive Ba^{2+} current was measured at 0 mV at the time the control current reached a peak. Inhibition was already detectable at agonist concentrations of 1–3 nM, increased with rising agonist concentration, and reached saturating levels at ~0.1–1 μM (Fig. 2 *A*). The IC_{50} was 9 nM, with Hill coefficient of 1.05 ($n = 42$).

With prolonged (>3 min) and/or repeated (more than five) applications of high concentrations (100 nM) of DPDPE, its inhibitory effect on Ba^{2+} current gradually desensitized. The rate of desensitization varied in different cells; however, the effects of DPDPE were invariably studied before desensitization began.

Voltage dependence of DPDPE inhibition

Ba^{2+} current inhibition by DPDPE occurred at all voltages tested, but it was greater for moderate depolarizations than for large depolarizations (Fig. 1, upper tracings). Maximal inhibition (>70%) was obtained by voltage steps negative to 0 mV. The degree of inhibition early in the pulse was greater than that at the end of the pulse, this being particu-

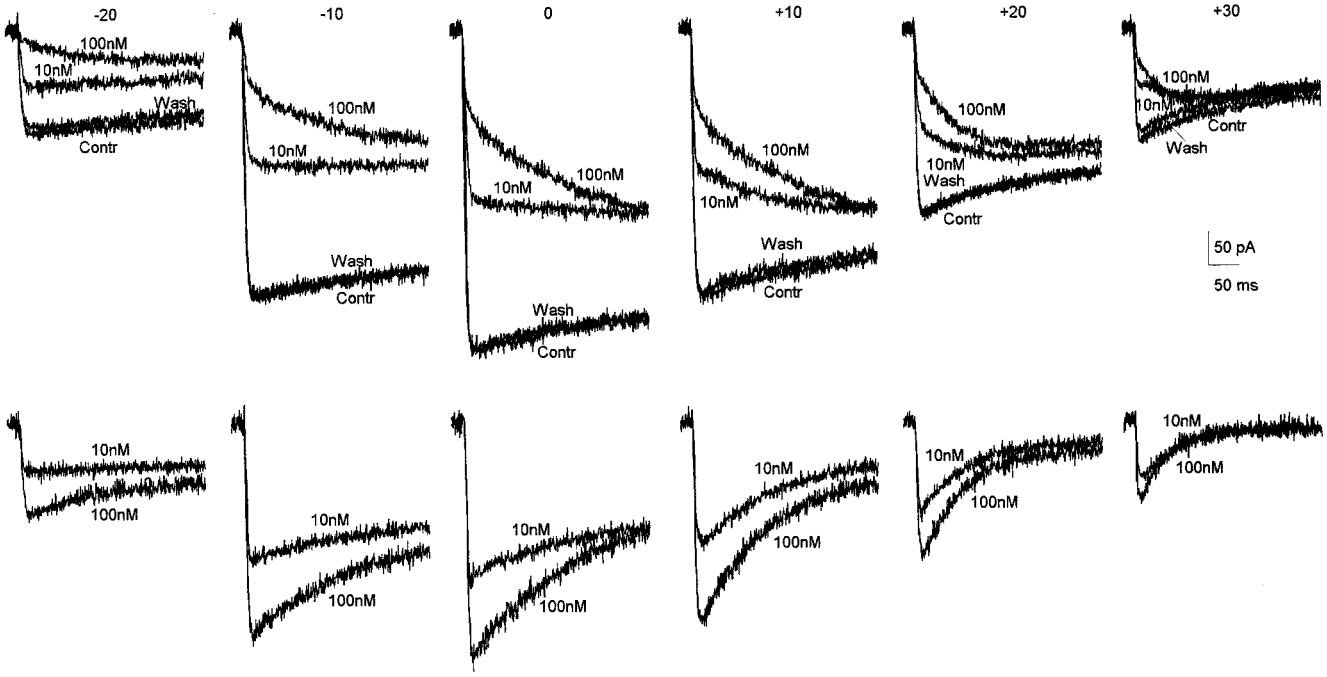

FIGURE 1 Inhibition of ω-CgTx GVIA-sensitive Ba^{2+} currents by DPDPE in NG 108-15 cells. (*Upper tracings*) Superimposed current traces were elicited to the potentials indicated during application of control saline (Contr), of 10 nM and 100 nM DPDPE, and after washout (Wash). (*Lower tracings*) Currents recorded in 10 and 100 nM DPDPE were subtracted from the control currents, recorded before agonist application. Holding potential was −40 mV.

larly evident with long lasting voltage steps positive to 0 mV. At each test potential, the time-dependent decrease in inhibition was related to a slowdown of current activation, as is evident from a simple inspection of the sample current tracings of Fig. 1 (upper tracings). A fast and a slow time constant could be measured from fits of agonist-modified current activation to the sum of two exponentials (not shown). However, observation of the control currents suggests that inactivation could complicate the measurements of the slow activation time constant (see upper sample tracings of Fig. 1). We tried to separate inactivation from slow activation by subtracting agonist-modified currents from control currents measured in the same cell (Fig. 1, lower tracings). This correction for inactivation should be a reasonable approximation if we assume that agonist-modified currents inactivate normally (Boland and Bean, 1993; Elmslie and Jones, 1994). To assess this point, Ba^{2+} current was measured at 0 mV from holding potentials ranging from −120 mV to −20 mV ($n = 3$) in cells lacking the LVA current component (~15–20% of tested cells). Indeed, as shown in Fig. 2 *B*, the voltage dependence of Ba^{2+} current inactivation was not dramatically altered during inhibition by DPDPE. The half-inactivation potential was shifted from −25.9 to −33.8 mV by 100 nM DPDPE. Also, the fraction of inhibited current measured at 0 mV was similar when starting from the different holding potentials of −120, −100, −80, −60, and −40 mV: 0.53, 0.53, 0.55, and 0.62, respectively. Thus, single-exponential fits to slow activation of control − DPDPE difference currents gave the values of slow time constants (τ_s). In a group of 18 cells, τ_s values were measured at different test potentials using two concentrations of DPDPE (10 and 100 nM). Between −10 mV and +30 mV, τ_s values were reduced more than eightfold by depolarization, and these values were similar at the two concentrations of agonist (Fig. 2 *C*). For instance, at 0 mV, τ_s was 207 ± 60 ms with 10 nM DPDPE and 220 ± 59 ms with 100 nM DPDPE. Thus, for currents elicited in the voltage range from −10 to +30 mV we did not find any evidence for concentration-dependent kinetics. Interestingly, however, at −20 mV, τ_s values of agonist-modified currents obtained with 10 nM DPDPE were significantly higher than those measured with 100 nM DPDPE (τ_s = 186 ± 34 ms and 148 ± 21 ms, respectively; *t*-test, confidence limit 0.05).

Relief and retrieval of inhibition

These preliminary results indicate a time- and voltage-dependent recruitment of ω-CgTx GVIA-sensitive Ca^{2+} channels from inhibition by DPDPE, i.e., channel de-inhibition. The degree of current de-inhibition at a fixed test potential should increase by applying depolarizing conditioning pulses of opportune amplitude and duration (Grassi and Lux, 1989). Fig. 3 A_{1-4} shows sample tracings of superimposed Ba^{2+} currents obtained under control conditions, during application of 10 or 100 nM DPDPE and during washout, by applying the protocol illustrated in Fig.

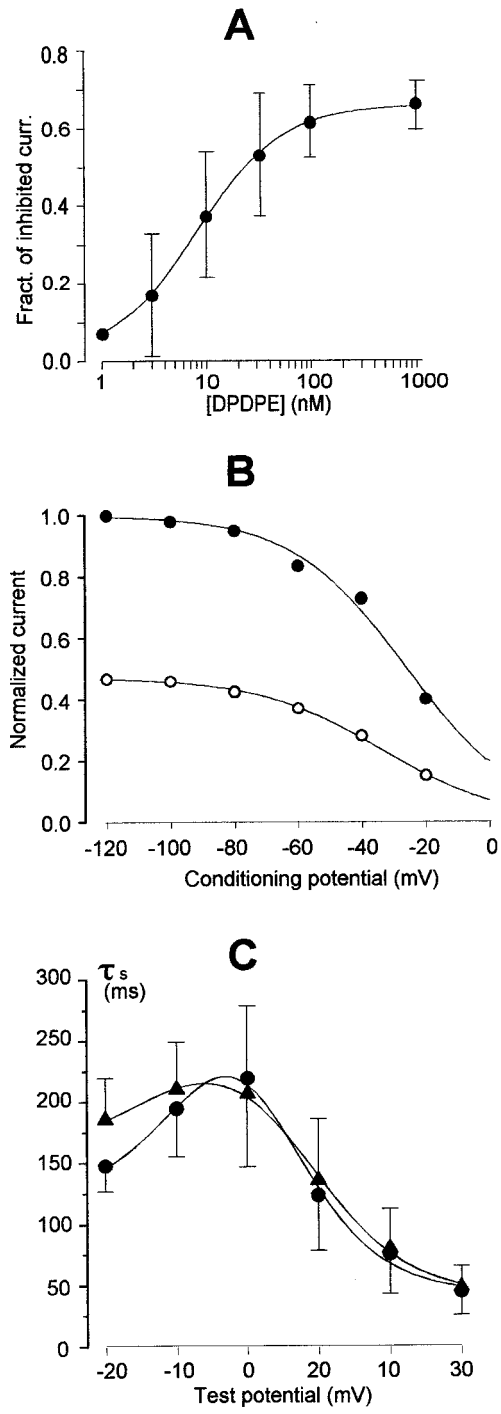

FIGURE 2 (*A*) Concentration dependence of DPDPE inhibition of Ba^{2+} currents. Measurements were made at test potentials that maximized Ba^{2+} currents (0/+10 mV). Symbols represent mean values from 42 cells. The continuous line is the fit of the data to the equation: $y = a/(1 + b/[\text{DPDPE}]^c)$ with $a = 0.66$, $b = 9$, and $c = 1.05$. (*B*) Effect of DPDPE on N-type Ba^{2+} current inactivation. Currents were elicited to 0 mV after a 3-s prepulse to the potentials indicated (−120/−20 mV). Protocols were run before (●) and during (○) application of 100 nM DPDPE, and currents were normalized to their largest values measured under control conditions at peak. The continuous lines through average data points ($n = 3$) are the least squares best fit of the Boltzmann type equation: $h_\infty = a/(1 + \exp((V + V_{1/2})/k))$ where $V_{1/2} = 25.9$ mV and $k = 17.9$ mV for control currents and $V_{1/2} = 33.8$ mV and $k = 19.4$ mV in the presence of DPDPE. (*C*) Voltage dependence of average slow time constants of activation ($n = 18$), measured during application of DPDPE 10 nM (▲) and 100 nM (●). τ_s was measured by single exponential fits to the slow component of the difference currents (control − DPDPE, lower sample tracings in Fig. 1). The continuous lines are the fit of data points to the equations $\tau_s = -407 + 449/\{1 + \exp[(V + 6)/-8]\} + 505/\{1 + \exp[\{V - 3)/7]\}$ (●) and $\tau_s = -394 + 429/\{1 + \exp[(V + 6.6)/ - 7.1]\} + 572/\{1 + \exp[\{V - 0.4)/8.6]\}$ (▲). Bars in *C* and *D* represent standard deviations.

3 *B*. Agonist-modified currents, which in the absence of conditioning pulses were depressed at the beginning of the test pulse to 0 mV (tracings labeled PS-40 in Fig. 3, A_2 and A_3), became larger by application of prepulses of increasing amplitude up to +80 mV (tracings labeled PS + 80 in Fig. 3, A_2 and A_3). By contrast, the test currents at 0 mV were not significantly affected by prepulses in the absence of DPDPE (Fig. 3, A_1 and A_4).

The average degree of de-inhibition ($n = 7$) of the DPDPE-modified current elicited during a test pulse to 0 mV versus prepulse potentials is shown in Fig. 3 *C* at two concentrations of DPDPE (10 and 100 nM).

After the strong recovery of current from agonist-induced inhibition, caused by sufficiently strong depolarizing prepulses and maximally detectable during the first tens of milliseconds of repolarization to the test pulse potential, the current relaxed slowly to a lower level, similar in amplitude to that reached in the absence of prepulse. This suggests that, although depolarization caused channel de-inhibition, channel re-inhibition occurred upon repolarization.

To compare directly the voltage dependence of Ca^{2+} channel re-inhibition with that of de-inhibition, the protocol illustrated in Fig. 4 was used: a depolarizing pulse to +80 mV, lasting 150 ms to maximally remove inhibition, preceded and followed by long test pulses of 600 ms. During a voltage step in the range of −20 to +30 mV, a fraction of the current activated rapidly. During DPDPE application, a slowly activating component of the current was also detectable, reflecting time- and voltage-dependent de-inhibition of the channels inhibited by the agonist, as already shown. After the conditioning pulse to +80 mV the current elicited by the test potential decreased biphasically; the early, rapidly deactivating current reflected the voltage-dependent closing at the repolarizing potential of a fraction of the channels opened by the conditioning pulse; under control conditions, the slowly relaxing current reflected exclusively channel inactivation whereas, in the presence of DPDPE, it reflected also time- and voltage-dependent channel re-inhibition (Fig. 4). The average fraction of current not inhibited at the end of both the prepulse and the postpulse (i.e., de-inhibited and re-inhibited current, respectively) is shown as a function of voltage in Fig. 5 *A*. Both sets of values were very similar, indicating that the same steady-state values could be reached with sufficiently long lasting prepulses and postpulses. These values were also consistent with those obtained using 100 nM DPDPE by applying the protocol shown in Fig. 3 *B* (see Fig. 3 *C*, closed circles).

Whether channel de-inhibition and re-inhibition proceed at the same or different rates was also assessed using the

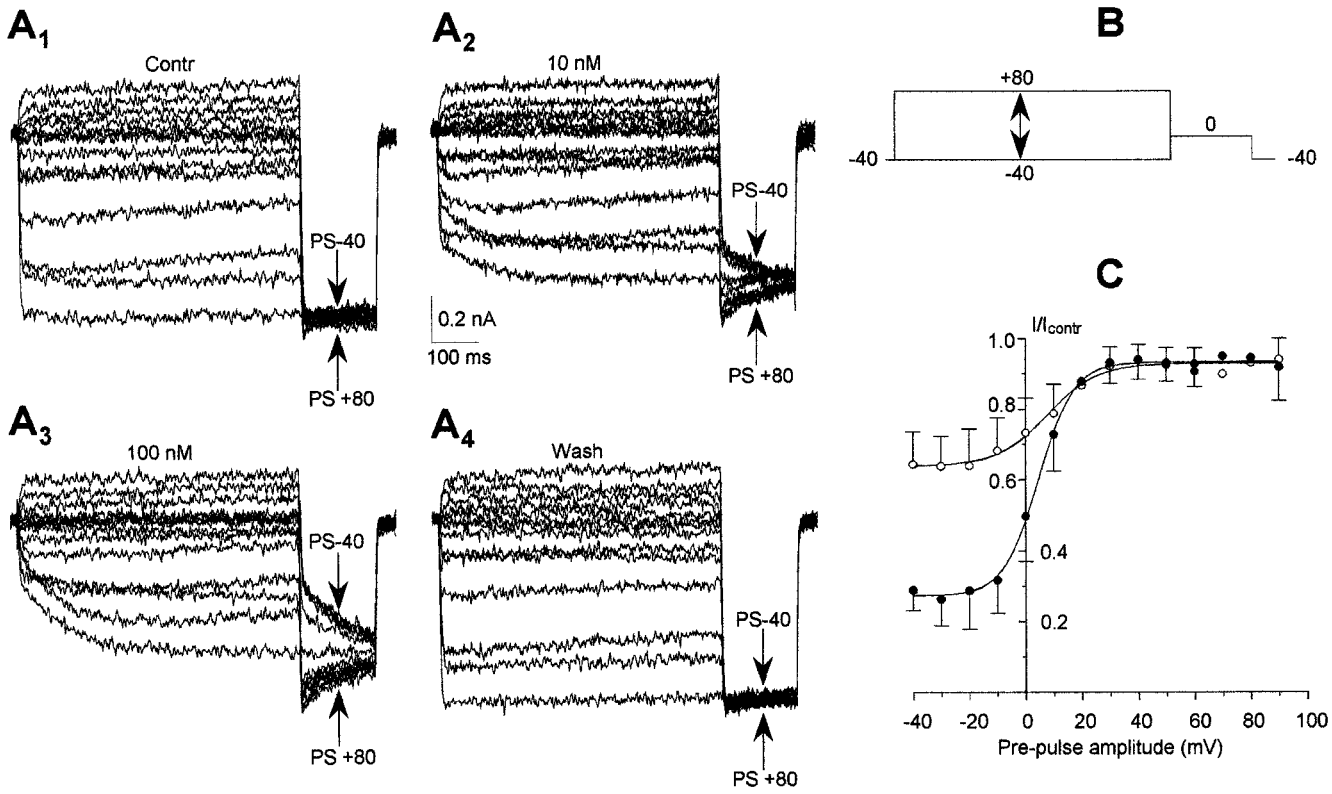

FIGURE 3 Effect of conditioning prepulses on DPDPE-modified Ba^{2+} currents. (A_{1-4}) Superimposed sample current traces elicited on step depolarization to 0 mV after a 600-ms conditioning prepulse of variable amplitude from −40 to +80 mV (protocol illustrated in *B*), with control saline (A_1), during application of 10 nM DPDPE (A_3) and 100 nM DPDPE (A_3), and after washout (A_4). (*C*) Voltage dependence of current deinhibition in DPDPE 10 nM (○) and 100 nM (●). Extent of de-inhibition was estimated by dividing the agonist modified current amplitude, measured a few tens of milliseconds after the test potential onset (indicated by arrows in the sample tracings), by the control current elicited without prepulse. Points and bars represent the means ± SD from seven cells. The continuous lines are the fit of data points to the equations $I/I_{contr} = 0.64 + 0.29/\{1 + \exp[(V - 7.8)/-8.9]\}$ (10 nM DPDPE) and $I/I_{contr} = 0.27 + 0.66/\{1 + \exp[(V - 4.6)/-6.3]\}$ (100 nM DPDPE). Bars in *C* represent standard deviations.

protocol illustrated in Fig. 4. Also in this case the slow kinetics of the two processes were measured from control − DPDPE difference currents to minimize contamination from current inactivation of the time constant measurements (sample tracings labeled diff in Fig. 4). Thus, slowly activating and slowly deactivating currents, elicited during each prepulse and postpulse, respectively, could be well fitted by single-exponential functions. In the voltage range from −20 to +30 mV, τ_s values of slow activation were invariably higher than those of slow deactivation (Fig. 5 *B*); the difference was statistically significant at −20, −10, 0, and +10 mV (*t*-test, confidence limit 0.05). For instance, at 0 mV the τ_s for de-inhibition (slow activation) was 220 ± 59 ms whereas the τ_s for re-inhibition (slow deactivation) was 145 ± 40 ms ($n = 18$). This indicates that the re-inhibition process was faster than that of de-inhibition in a wide voltage range.

Recovery of inhibition upon strong repolarization

The time course of re-inhibition during strong repolarizations was studied as well at two different concentrations of DPDPE (10 and 100 nM). The protocol shown on the top left corner of Fig. 6 *A* was used. The top left current records in Fig. 6 *A* show that in the absence of agonist the magnitude of the Ba^{2+} current was stable and not altered by the prepulse protocol. By contrast, during DPDPE application, the current, reduced in amplitude and slowly activating during the first test pulse, increased significantly during the second test pulse because of channel de-inhibition. However, the current amplitude measured during the second test pulse decreased gradually by increasing the duration of the repolarizing interpulse to −40 mV. Current magnitude approached the value evoked by the first test pulse (i.e., full re-inhibition occurred), for long-lasting repolarizing interpulses (Fig. 6 *A*, upper right tracings (10 nM DPDPE) and lower left tracings (100 nM DPDPE)).

The average data obtained from 13 cells, where 10 and 100 nM DPDPE was applied in train on each cell, show that the rate of re-inhibition increased with increasing agonist concentration (Fig. 6 *B*). The onset of re-inhibition at −40 mV could be approximated by a single exponential. The mean time constants of re-inhibition (τ_r), obtained from averaging τ_r values determined separately for each of the 13 cells examined, were 132 ± 12 ms and 76 ± 7 ms for 10 and 100 nM DPDPE, respectively. By applying a similar

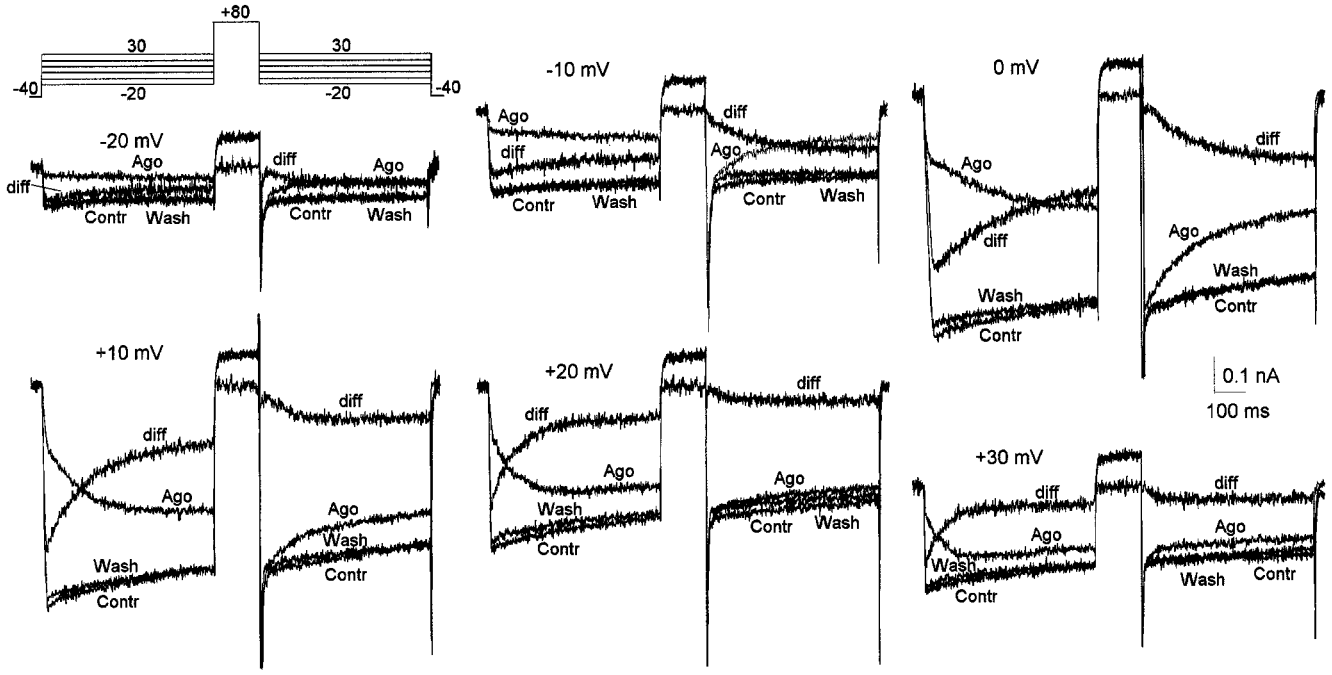

FIGURE 4 Slow activation and slow deactivation kinetics during opioid application. Superimposed sample tracings were elicited to the test potentials indicated before and after a conditioning pulse to +80 mV (protocol shown in the upper left corner) in the presence of control saline (Contr), during application of 100 nM DPDPE (Ago), and after washout (Wash); tracings labeled diff represent the difference currents (control − DPDPE). Holding potential was −40 mV.

protocol to cells lacking the LVA current component, τ_r values could be calculated also for repolarizations to −60 mV in 100 nM DPDPE ($n = 6$) and to −80 mV in 100 nM and 10 nM DPDPE ($n = 9$). τ_r values are plotted as a function of the repolarization potentials in Fig. 6 *C*. The difference between τ_r measured at −40 mV and −80 mV was statistically significant between 10 and 100 nM DPDPE (*t*-test, confidence interval 0.05) and indicates a dependence of re-inhibition kinetics on agonist concentration at these potentials. Surprisingly, Kasai (1992) did not observe a

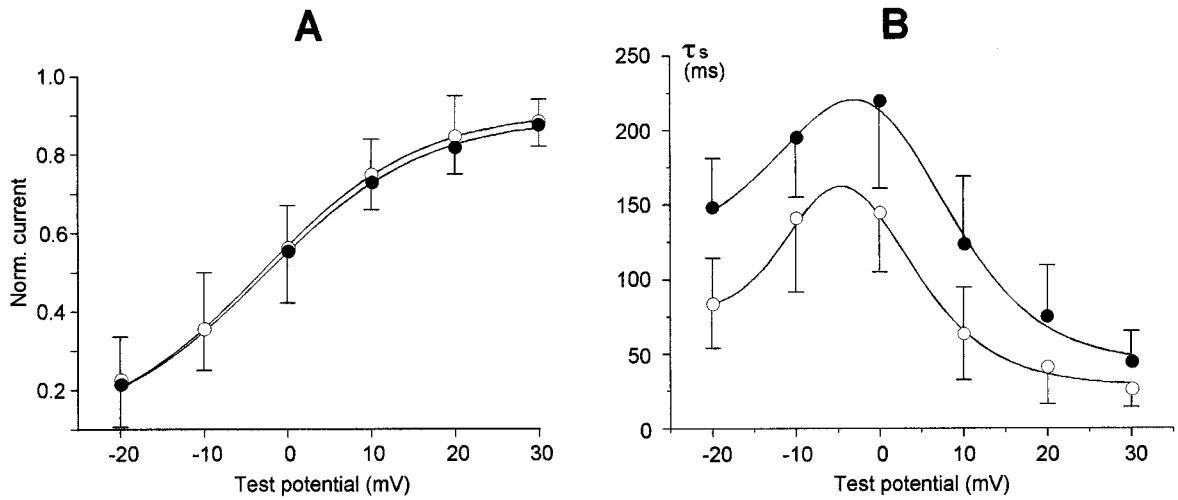

FIGURE 5 Voltage and time dependence of relief and retrieval of inhibition in the presence of 100 nM DPDPE. (*A*) Normalized current values at the end of the test potentials before the conditioning pulse (●) and after the conditioning pulse (○) were obtained by dividing the DPDPE-modified currents by the controls and plotted as a function of test potentials. The continuous lines are the fits of data points to the equations $I/I_{contr} = 0.09 + 0.81/\{1 + \exp[(V + 3.0)/-9.7]\}$ (●) and $I/I_{contr} = 0.09 + 0.82/\{1 + \exp[(V + 3.2)/-9.5]\}$ (○). (*B*) Time constants of slow activation (●) and slow deactivation (○) were measured by single exponential fits to the slow component of the control − DPDPE currents (sample tracings labeled diff in Fig. 4) and plotted against test potentials. The continuous lines are the fits of data points to the equation $\tau_d = -407 + 449/\{1 + \exp[(V + 6)/-8]\} + 505/\{1 + \exp[\{V - 3)/7]\}$ (●) and $\tau_r = -414 + 442/\{1 + \exp[(V + 8.4)/-4.5]\} + 497/\{1 + \exp[\{V - 4)/6]\}$ (○). Data points in *A* and *B* are averages from 18 cells. Bars in *A* and *B* represent standard deviations from the mean.

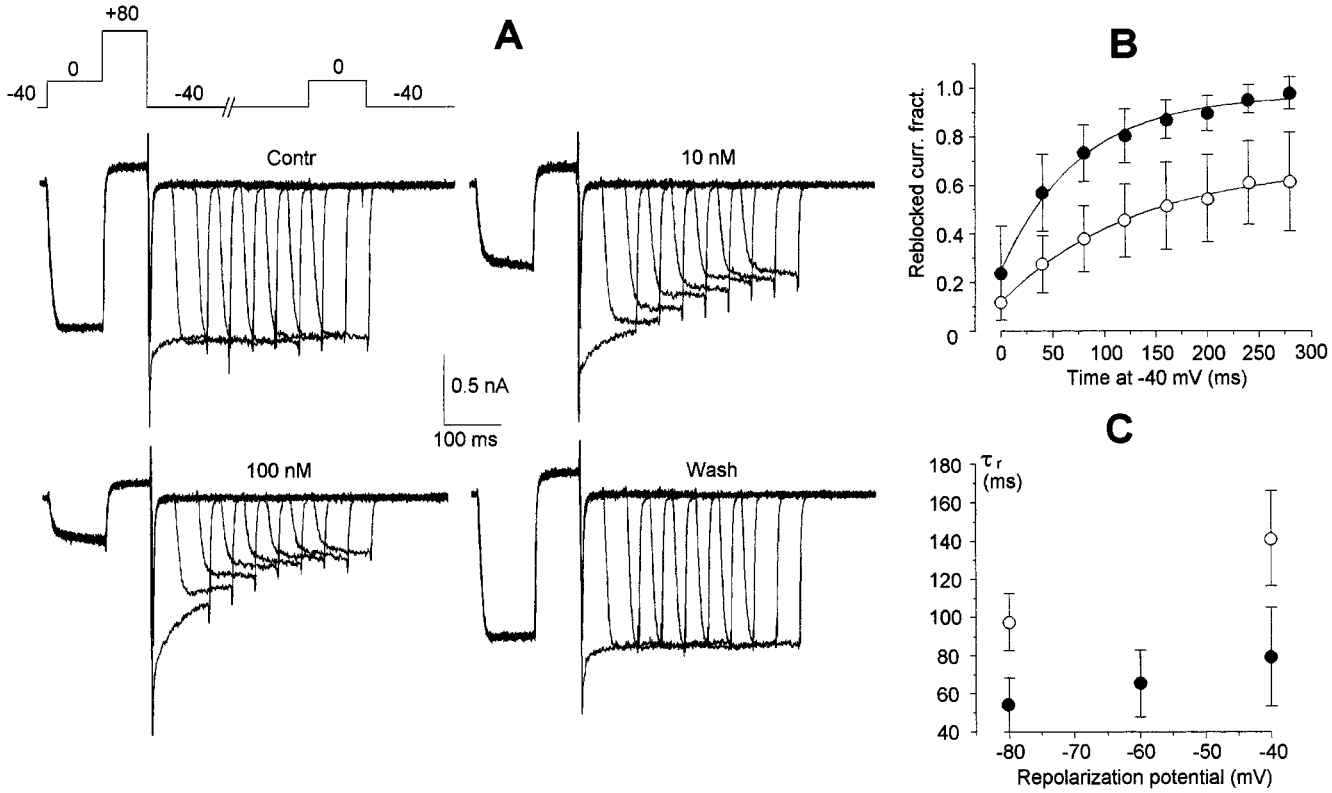

FIGURE 6 Time course of re-inhibition at negative potentials. (*A*) Superimposed Ba^{2+} currents recorded at the test pulse of 0 mV before and after an 80-ms prepulse to +80 mV, followed by an interpulse to −40 mV of variable duration (0–280 ms) (protocol on the top left corner), in the presence of control saline (upper left traces), for 10 nM DPDPE (upper right traces) and 100 nM DPDPE (lower left traces) and after washout (lower right traces). The following protocol was used (top left corner): Ca^{2+} channel current was first elicited with a test pulse to 0 mV for 90 ms from a holding potential of −40 mV. The membrane was then stepped to +80 mV for 75 ms, which allowed for maximal de-inhibition, and repolarized to −40 mV for a variable time. The extent of re-inhibition was finally assayed by a second test pulse to 0 mV. (*B*) Fraction of re-inhibited current as a function of the duration of the repolarizing pulse at DPDPE concentrations of 10 nM (○) and 100 nM (●). The fraction of re-inhibited current for each repolarization interval was estimated by subtracting the DPDPE-modified current from the control current and dividing the difference by the control current; current amplitudes were measured ~20 ms after the onset of the second test pulse. Points and bars are means ± SD (n = 13). The continuous lines in *B* are the best fits of data points to single exponential functions; time constants are 76 ms (100 nM DPDPE, ●) and 132 ms (10 nM DPDPE, ○). (*C*) Time constants of re-inhibition (τ_r) for 100 nM DPDPE (●) and 10 nM DPDPE (○) plotted as a function of repolarization potentials. Bars in *B* and *C* represent standard deviations.

significant concentration dependence of re-inhibition of Ca^{2+} channel current at −40 mV by DPDPE in NG108-15 cells. Apart from the fact that it is not clear whether in that case the two different concentrations of agonist were applied in train on each cell tested, as we did, or separately on different cells (in which case τ_r measurements could have been biased), we do not have any explanation for this discrepancy. The rate of re-inhibition could be an important parameter to understand whether facilitation could occur in physiological conditions, such as during a train of action potentials (see below).

Relief from inhibition upon strong depolarization

We have previously seen that the time constant of de-inhibition τ_s decreased monotonically in the voltage range between 0 and +30 mV. The time course of de-inhibition at more depolarizing voltages, positive to +40 mV, was studied using the following protocol: Ba^{2+} currents were elicited during a test pulse to 0 mV after depolarizing prepulses of variable duration (0–70 ms). This protocol and an example of the effect on Ca^{2+} channel current of prepulse duration at +80 mV is shown in Fig. 7 *A*. Increasing the duration of the prepulse during application of 100 nM DPDPE produced de-inhibition (lower tracings in Fig. 7 *A*). The same protocol did not produce any significant effect on Ba^{2+} current in the absence of agonist (upper tracings in Fig. 7 *A*).

Mean de-inhibition time courses at +40 mV (n = 5), +80 mV (n = 5), and +120 mV (n = 4) against prepulse duration are shown in Fig. 7, *B–D*. Onsets of de-inhibition at each prepulse potential could be approximated by single-exponential curves whose time constants τ_s are plotted against prepulse amplitude in Fig. 7 *E*. In the voltage range from +40 mV to +120 mV τ_s decreased exponentially from 14.1 ± 1.1 ms to 6.6 ± 0.5 ms.

These results show that development of de-inhibition reached a limiting time constant of ~7 ms for very large depolarizations. Whether channel de-inhibition and activation have similar or different rates is a very important point to distinguish different models of N-type Ca^{2+} channel

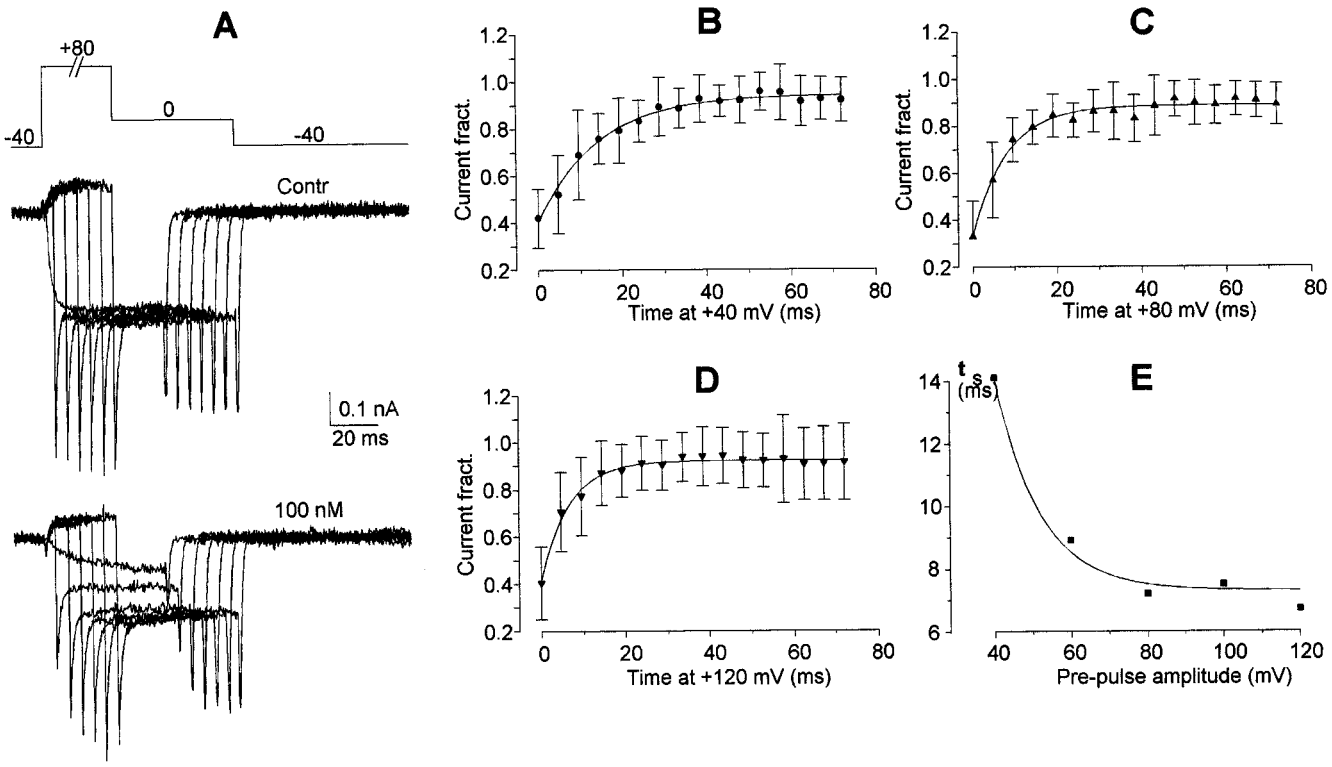

FIGURE 7 Onset of relief of inhibition at large depolarizations. (*A*) Superimposed Ba^{2+} current traces recorded at 0 mV after a prepulse to +80 mV of variable duration (0–72 ms) before and during application of DPDPE 100 nM (upper and lower tracings, respectively). (*B–D*) Relationship between mean de-inhibition and prepulse duration at +40 mV ($n = 5$), +80 mV ($n = 5$), and +120 mV ($n = 4$), as indicated by labels. The fraction of de-inhibited current for each prepulse duration was measured by dividing the DPDPE-modified current by the control current, measured ~20 ms after the onset to the test potential. Data points and bars are means ± SD from seven cells. The continuous lines in *B, C*, and *D* are the best fits of the data points to an equation of the type $a - (a - b)\exp(-t/\tau$; the time constants are 14.1 ms (+40 mV), 8.1 ms (+80 mV), and 6.6 ms (+120 mV). (*E*) Time constants of de-inhibition (measured as shown in *B–D*) as a function of prepulse amplitude. The solid line is described by the equation $\tau_d = -424 + 442/\{1 + \exp[(V + 148)/-0.04]\} + 425/\{1 + \exp[\{V + 8.9)/11.6]\}$.

inhibition (Boland and Bean, 1993). Therefore, to compare the kinetics of de-inhibition with the rate of activation after depolarization to very positive potentials in the presence of DPDPE, the time course of Ca^{2+} channel activation was studied as follows: tail currents at −40 mV were measured after conditioning pulses of variable duration to +80 mV. Fig. 8 *A* shows superimposed tail current tracings obtained under control conditions and during cell perfusion with 100 nM DPDPE by applying the protocol shown on top. On average, control tail currents reached almost maximal values after ~1 ms depolarization to +80 mV (Fig. 8 *B*, open circles). By contrast, in the presence of agonist, the tail current was only 41% of maximum after 1 ms to +80 mV and 86% of maximum after 21 ms (Fig. 8 *B*, closed circles). Like at lower test potentials (see Fig. 1), also the time course of activation at +80 mV is clearly biphasic, with rapid (conditioning range, 0–1 ms; $\tau < 1$ ms) and slow (conditioning range, 1–21 ms) components. Best fitting of the time course of slow activation at +80 mV in the presence of DPDPE was obtained with a single-exponential function, which gave a time constant of 7.4 ± 1.3 ms. As shown in the example tracings of Fig. 8 *C*, similar time constants for slow activation were also obtained in three experiments where the kinetics of activation was studied at +120 mV (6.8 ± 0.9 ms). At +120 mV a large outward current carried by Cs^+ ions through open Ca^{2+} channels was also evident. The tracings in Fig. 8 *C* show that the activation kinetics measured from the time courses of the outward currents and peak tail currents are very similar under control conditions ($\tau < 1$ ms in both cases), both of them becoming biphasic with similar slow components with agonist ($\tau = 5.5$ and 5.3 ms respectively).

These data indicate that slow activation of agonist-modified channels is a process indistinguishable from de-inhibition, both of them reaching similar limiting time courses even at very strong depolarizations.

Some authors found that, in the presence of agonist, tail current decay after short conditioning pulses was faster than the decay of control tail currents and of those after long-lasting depolarizations in the presence of agonist (Elmslie et al., 1990; Pollo et al., 1992; Boland and Bean, 1993). Whether the kinetics of the tail current changed during the time that de-inhibition occurred is another crucial point for distinguishing different models of channel modulation.

To assess this point, tail current relaxation was fitted with single exponentials. The rate of tail currents in the presence

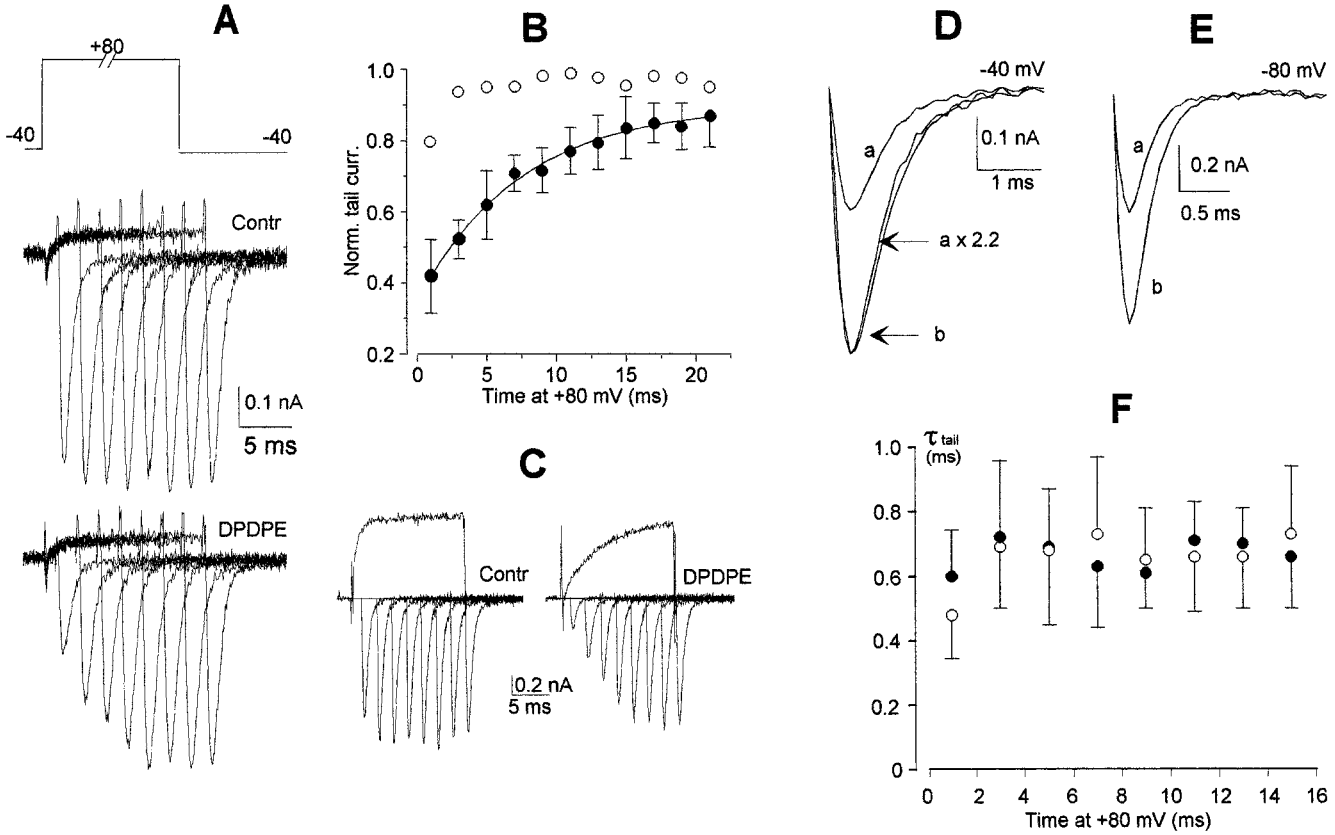

FIGURE 8 Effect of DPDPE on activation of N-type Ca^{2+} channel current. (*A*) Sample tail currents at −40 mV in the absence (traces on the left) or presence (traces on the right) of 100 nM DPDPE after pulses to +80 mV of variable duration (1–15 ms) (protocol shown on top). (*B*) Time course of activation in the absence (○) and in the presence (●) of DPDPE. The fraction of activated channels during each pulse to +80 mV was obtained by dividing the tail current after the pulse by the maximal tail current obtained in the control. The activation values were then plotted as a function of the pulse duration. Data points and bars are mean values ± SD from three cells. The solid line is the best fit of the data points to a single exponential; the time constant is 7.4 ms. (*C*) Sample tail currents at −40 mV in the absence (traces on the left) or presence (traces on the right) of 100 nM DPDPE after pulses to +120 mV of variable duration (1–15 ms). (*D*) Traces labeled *a* and *b* in *A* are shown on an expanded time scale; trace *a* is also scaled up to match the peak amplitude of trace *b*. (*E*) Sample tail currents at −80 mV obtained in the presence of 100 nM DPDPE and from the same cell as in *B* after pulses to +80 mV lasting 1 ms (*a*) and 15 ms (*b*). τ_{tail} values were 0.20 and 0.21 ms, respectively. (*F*) Time constants of tail current relaxation, plotted as a function of pulse duration at +80 mV, before (○) and during (●) DPDPE application. τ_{tail} values were obtained by fitting tail currents with single exponential functions. Bars in *E* represent standard deviations.

of 100 nM DPDPE varied negligibly after conditioning prepulses of duration between 1 and 15 ms, as made evident in Fig. 8 *D* by scaling the tail after a 1-ms prepulse (trace a: τ_{tail} = 0.61 ms) to match the peak size of the tail after a 15-ms prepulse (trace b: τ_{tail} = 0.65 ms). The average values (n = 4) of these time constants measured in the absence or presence of agonist after prepulses of variable duration (from 1 to 15 ms) are plotted as a function of prepulse duration in Fig. 8 *F*. Our results show no sizeable changes in repolarization kinetics after pulses of variable duration to +80 mV in the presence of DPDPE. Also, the time course of current repolarization in the presence of agonist was similar to that measured in control saline. One additional test on the accuracy of tail current measurements was done by measuring tail currents at potentials more negative than −40 mV. Fig. 8 *E* shows example tracings of tail currents elicited at −80 mV after prepulses to +80 mV lasting 1 ms (a) and 15 ms (b) in the presence of DPDPE. As expected, they show a faster time course than those obtained at −40 mV (Fig. 8 *D*). On the average we measured a τ_{tail} of 0.21 ± 0.01 ms on repolarization to −80 mV (n = 3).

Model simulation of ω-CgTx GVIA-sensitive Ca^{2+} channel inhibition

A minimal model that fits our experimental results assumes that an inhibitory molecule interacts in a voltage-dependent manner with closed states of the channel to give modulated, nonconducting conformations. Modulated (inhibited) states are supposed to equilibrate with a normally closed state through voltage-dependent rate constants that are rate limiting for channel activation even at strong membrane depolarizations:

$$B_1 \underset{r_1}{\overset{d_1}{\rightleftarrows}} B_2 \underset{r_2}{\overset{d_2}{\rightleftarrows}} C \underset{b}{\overset{a}{\rightleftarrows}} O$$

States B_1 and B_2 represent inhibited closed states to which channels are moved at rest when a certain amount of the

inhibitory molecule (presumably an activated G protein) is present and from which they are slowly removed during depolarization. It is assumed that in states B_1 and B_2 the inhibitory molecule is bound to the channel. The inclusion of two binding sites in the model takes into account the experimental observation that slow activation is faster than slow deactivation. State C is a normal closed state of the channel without inhibitory molecule bound and to which channels are moved by depolarization. State O is the open state, with the inhibitory molecule unbound from the channel. According to this model, a and b, the normal forward and backward activation rates, and the rate constants of de-inhibition d_1 and d_2 are strongly voltage dependent; re-inhibition rate constants r_1 and r_2 are assumed to be both voltage and concentration dependent.

The parameters of the model were adjusted by trial and error to give a reasonable approximation of channel voltage dependence and gating kinetics. The estimated rate constants of de- and re-inhibition that best fitted experimental data could be approximated by the following expressions (in s^{-1}):

$$d_1 = 1229(84 - V)/\{\exp[(84 - V)/7.9] + 6.0(84 - V) - 1\} + 8.4/\{1 + \exp[(V - 2)/20.1]\}$$

and

$$d_2 = 2201(91 - V)/\{\exp[(91 - V)/8.1] + 10.4(91 - V) - 1\} + 5.5/\{1 + \exp[(V - 3)/23.5]\}$$

at any concentration of agonist;

$$r_1 = 1129(127 - V)/\{\exp[(127 - V)/9.1] + 154(127 - V) - 1\} + 13.3/\{1 + \exp[(V + 21)/14.8]\}$$

and

$$r_2 = 192(108 - V)/\{\exp[(108 - V)/8.8] + 56(108 - V) - 1\} + 8/\{1 + \exp[(V + 11)/17.4)\}$$

at saturating concentrations of agonist.

In our model, saturable rates of re-inhibition were necessary to reproduce the observed incomplete inhibition. Therefore, it was assumed that r_1 and r_2 are nonlinear functions of DPDPE concentration. This implies a deviation of the model from bimolecular kinetics. Therefore, the multiplication factor that takes into account the dependence of r_1 and r_2 from agonist concentration, i.e., the fractional occupancy of DPDPE receptors, is [DPDPE]/(9.9 + [DPDPE] (with nanomolar [DPDPE]). The rate constants of fast activation and deactivation have the following expressions (in s^{-1}):

$$a = 1682/\{1 + \exp[(V - 19.0)/ - 15.1]\}$$

and

$$b = 1663/\{1 + \exp[(V + 29.7)/8.9]\}.$$

For the sake of simplicity, Ca^{2+} channel inactivation was not implemented in the model, and only one normal closed state was considered, although fast activation of N-type Ca^{2+} channel current is best described by m^2 kinetics in NG108-15 cells (Kasai and Neher, 1992).

The reliability of this model was tested by simulating the main features of the inhibitory action of the agonist on a population of ω-CgTx GVIA-sensitive channels. The occupancy of different states of the model was calculated using Runge-Kutta integration with a time step of 1/400 of the time range examined. The driving force for open channels was assumed to obey the Goldman-Hodgkin-Katz equation with $E_{Ba} = +60$ mV.

During simulation, control tracings did not show a slow activation component at any voltage (Fig. 9 *A*). By contrast, agonist-modified currents activated after step depolarizations with a time course that was biphasic (Fig. 9, *B* and *C*), in good agreement with experimental results. The slow time constant of activation, τ_s, reached a maximum at ~ -10 mV both at the saturating agonist concentration (1 μM) and at the 10 nM concentration (Fig. 9 *F*). At -20 mV and 10 nM agonist, τ_s increased ~17% in comparison with the 1 μM concentration (324 and 269 ms, respectively), similarly to experimental observations. Positive to $+20$ mV, τ_s values became similar at both agonist concentrations; for instance, during simulation, τ_s values obtained at $+30$ mV were 29 and 27 ms, respectively, also in agreement with experimental results. However, it must be pointed out that at 0 mV our model predicts a sizable decrease in τ_s for a 100-fold decrease in agonist concentration (τ_s = 347 and 275 ms at 1 μM and 10 nM, DPDPE respectively), whereas no significant change in τ_s was observed experimentally at the two agonist concentrations. This point will be discussed further below.

The experimental observation that the time course of re-inhibition was faster than that of de-inhibition in a wide range of depolarizing potentials was well implemented by the two adjacent inhibited states in the kinetic scheme. By applying the same protocol shown in Fig. 4 we obtained the simulated currents shown in Fig. 9 *D* at a saturating concentration of agonist. Starting from a holding potential of -40 mV, τ_s values during de-inhibition measured at -20, 0, and $+20$ mV were 269, 347, and 61 ms, respectively, whereas τ_s values measured at the same potentials after a prepulse to $+80$ mV, i.e., during re-inhibition, were 188, 229, and 53 ms, respectively. Positive to 0 mV the model predicts a less prominent re-inhibition than experimental data.

Fig. 9 *E* shows the simulated dose-response relationship (EC_{50} = 4.7 nM), which mimics the experimental curve reported in Fig. 2 *A*. The model predicts incomplete inhibition at saturating concentrations of agonist, in agreement with experimental results.

Fig. 10 *A* shows the voltage dependence of de-inhibition at two different concentrations of agonist, studied as in Fig. 3. Both sets of data were fitted with equations of the form $a + b/\{1 + \exp[(V - V_{1/2})/k]\}$, with $V_{1/2} = -15.8$ *mV* and

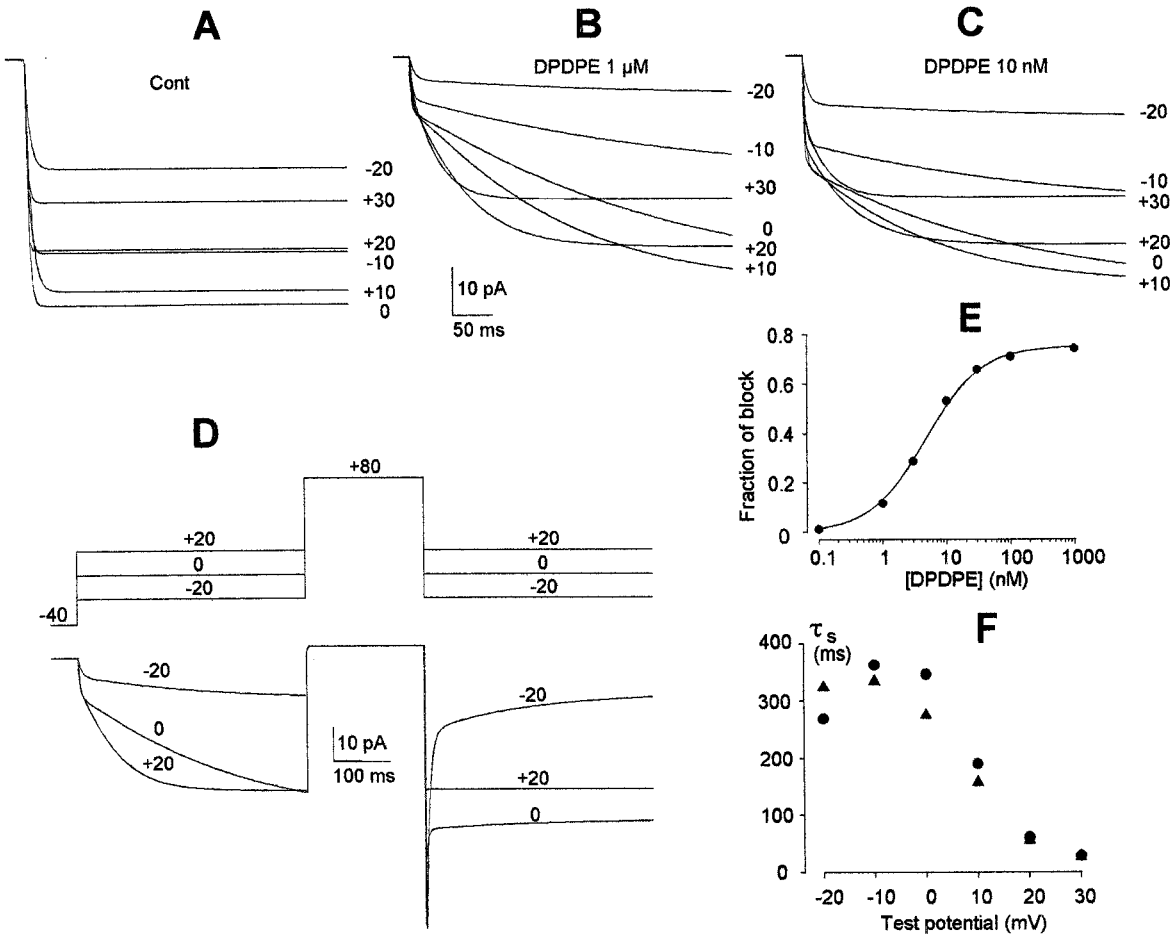

FIGURE 9 (*A–C*) Computer simulation of N-type Ca^{2+} channel current time course at the test potentials indicated, either under control conditions (*A*) or in the presence of an agonist concentration of 100 or 10 nM (*B* and *C,* respectively), using the kinetic model illustrated in the text. The slow phase of activation to −20, −10, 0, +10, +20, and +30 mV has a τ_s of, respectively, 269, 363, 347, 190, 61, and 29 ms in the presence of a saturating concentration of agonist (100 nM) and a τ_s of, respectively, 324, 334, 275, 157, 55, and 27 ms in the presence of a 10-fold lower agonist concentration (10 nM). (*D*) Simulation of the time courses of N-type Ca^{2+} current de-inhibition and re-inhibition at the test potentials indicated and in the presence of a saturating agonist concentration. τ_d = 269, 347, and 61 ms at −20, 0, and +20 mV, respectively. τ_r = 188, 229, and 53 ms at −20, 0, and +20 mV, respectively. (*E*) Simulated dose-response relationship determined using simulated 12-ms depolarizations from −40 mV to 0 mV. Solid line is drawn according to the equation $y = 0.75/(1 + 4.7/[\text{DPDPE}])$. (*F*) Voltage dependence of the slow time constants of activation τ_s, measured by single exponential fits to the slow component of the simulated currents in *B* (●, 1 μM DPDPE) and in *C* (▲, 10 nM DPDPE).

−18.8 mV and k = −6.1 and −8.2 mV for 1 μM and 10 nM agonist concentrations, respectively. A shift of ~10 mV in voltage dependence between the model and experimental data is evident. It should be noted that the model predicts 100% recovery from inhibition. The incomplete recovery observed experimentally even at strong depolarizations (~90% maximal recovery; see Fig. 3 *B*) is probably due to current inactivation occurring during the long-lasting conditioning pulses preceding the test pulse.

Fig. 10 *B* shows the simulated time courses of re-inhibition during repolarization to −40 mV for agonist concentrations of 1 μM and 10 nM, studied as in Fig. 6. The time constant of re-inhibition at saturating concentrations of agonist was 130 ms and increased to 178 ms by a 100-fold decrease in agonist concentration.

The simulation of the time course of activation at strong depolarizing potentials was obtained using the same protocol shown in Fig. 7 (Fig. 10 *C*). In the presence of agonist, the rate of activation reached a limiting time constant of 7.9 ms for a depolarization to +80 mV (τ = 7.8 ms at +120 mV), which was indistinguishable from the time constant for de-inhibition, measured by simulating the protocol shown in Fig. 8 *A* (τ = 7.9 ms). The simulated tail currents in the inset of Fig. 10 *C* show that the model also accounts for the similar kinetics of the tail currents that follow short depolarizations (2 ms) or long depolarizations (20 ms) to very positive potentials (τ_{tail} = 0.76 ms in both cases).

Finally, the model was used to simulate Ca^{2+} channel de-inhibition in response to a train of depolarizing pulses that roughly mimic a burst of action potentials (Williams et al., 1997). The model predicted ~38% de-inhibition by simulating a re-inhibition time constant of 80 ms, corresponding to that measured experimentally with 100 nM DPDPE, and 63% deinhibition was obtained by simulating

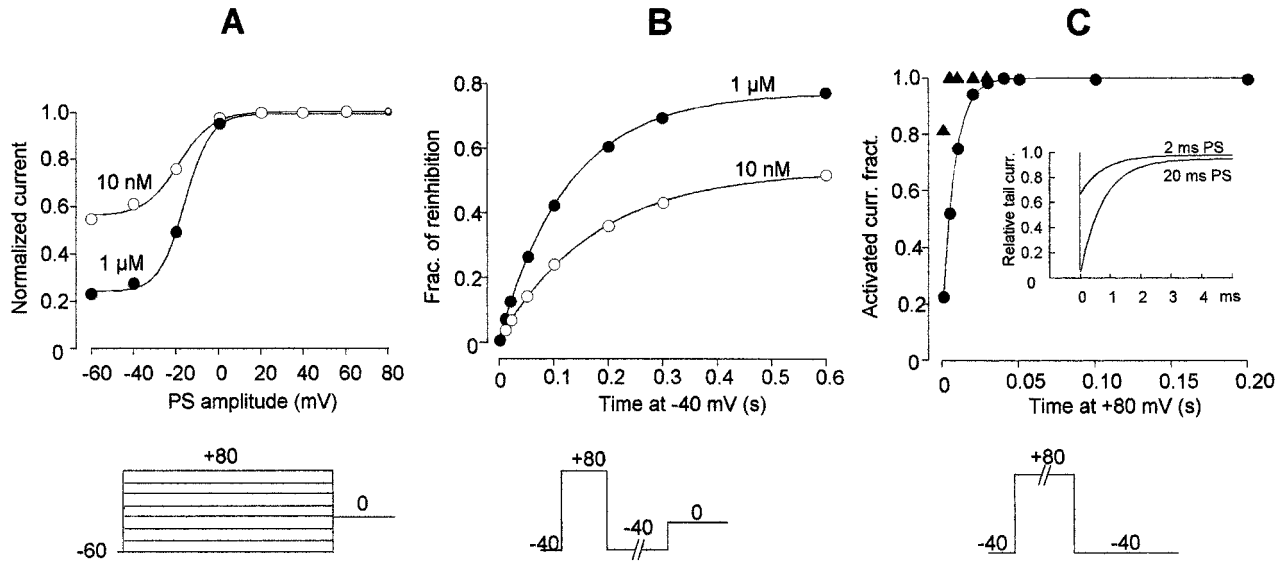

FIGURE 10 (*A*) Simulated voltage dependence of Ca^{2+} current de-inhibition at a saturating agonist concentration (1 μM) and at a 100-fold lower concentration (10 nM). Data points, estimated as in Fig. 3 *C*, represent the extent of de-inhibition and were obtained by applying the bottom protocol. They were fitted with functions of the form $0.56 + 0.44/\{1 + \exp[(V + 18.8)/-8.2]\}$ (10 nM) and $0.25 + 0.75/\{1 + \exp[(V + 15.8)/-6.1]\}$ (1 μM). (*B*) Simulated onset of re-inhibition at -40 mV and at agonist concentrations of 1 μM and 10 nM. Data points were obtained simulating the protocol shown on the bottom. The time constants of re-inhibition, obtained by fitting data points with single exponential functions, were 130 ms (●) and 178 ms (○), respectively. (*C*) Simulation of the time course of Ca^{2+} current activation at $+80$ mV in the presence of a saturating concentration of agonist (●) and in the absence of agonist (▲). Data points were obtained from peak tail current amplitudes simulating the protocol shown on the bottom. Data points indicated by circles are fitted with a single exponential function ($\tau = 7.9$ ms). (*Inset*) simulated tail currents at -40 mV after pulses to $+80$ mV of 2- and 20-ms duration, as indicated by labels.

a re-inhibition time constant of 130 ms, corresponding to that measured experimentally with 10 nM DPDPE. By contrast, de-inhibition was reduced to only 8% by simulating a re-inhibition time constant of 30 ms. This result predicts that sizeable de-inhibition could be effectively evoked by physiological stimuli, and its extent would depend, besides other factors, on the rate of channel re-inhibition.

DISCUSSION

Comparison with previous results

Our results, obtained using differentiated NG108-15 cells and the δ-opioid agonist DPDPE, show that inhibition of N-type Ca^{2+} channel current caused by membrane receptor activation is voltage and time dependent, occurring most effectively at negative membrane potentials and being relieved by depolarization (Marchetti et al., 1986; Bean, 1989; Grassi and Lux, 1989; Elmslie et al., 1990; Lopez and Brown, 1991; Kasai, 1992; Pollo et al., 1992; Golard and Siegelbaum, 1993; Toselli et al., 1995).

In the voltage range between -20 and $+30$ mV de-inhibition and re-inhibition proceed at different rates in the presence of DPDPE (Fig. 5 *B*). Namely, the rate of re-inhibition is faster than that of de-inhibition measured at the same test potential. This result brings new insights into the behavior of the modulated N-type Ca^{2+} channel, suggesting that multiple blocked states co-exist when channels are bound to the inhibitory molecules. De-inhibition kinetics was independent from agonist concentration at test potentials positive to -10 mV, whereas a concentration dependence was observed at the test potential of -20 (Fig. 2 *C*), in contrast with other reports (Kasai, 1992; Pollo et al., 1992; Elmslie and Jones, 1994). A plausible explanation could be that changes in membrane potential cause unbinding and rebinding of a modulatory molecule with the Ca^{2+} channel. Indeed, considering this binding/unbinding process as a second (or greater) order reaction during which the channel can pass between inhibited and not inhibited states, changes in the concentration of the inhibitory molecule should affect the time course of the reaction.

Also, re-inhibition kinetics after repolarization to negative potentials was both voltage and concentration dependent. The authors who previously investigated this point reported contradictory results (Lopez and Brown, 1991; Kasai, 1992; Golard and Siegelbaum, 1993; Elmslie and Jones, 1994; Ehrlich and Elmslie, 1995; Zhou et al., 1997). For instance, Kasai could not observe concentration dependence of re-inhibition kinetics at -40 mV. In sympathetic neurons, instead, Elmslie and Jones (1994) observed a concentration dependence of the time course of re-inhibition during repolarization to -80 mV, but in that case no quantitative measurement of the time constants of re-inhibition was reported as the time course of re-inhibition could not be well fitted by a single exponential. We found that the time constant of re-inhibition decreased both by increasing ago-

nist concentration and by decreasing the repolarization potential.

The rate of de-inhibition speeded up considerably at very positive potentials, reaching a limiting value between +80 mV and +120 mV ($\tau_d \approx 7$ ms) that during application of DPDPE was similar to the time course of the slow component of Ca^{2+} channel activation. Both processes were much slower than channel activation under control conditions (<1 ms). However, it is noteworthy that even at saturating agonist concentrations a fraction of the current (20–40%) activated as fast as control current, so that current activation was always biphasic. Fast activation could reflect incomplete inhibition; i.e., a channel fraction is not affected by the agonist and therefore activates as fast as under control conditions. Indeed, inhibition was never complete. By contrast, the slow activating component would reflect activation of agonist-modified channels, a process indistinguishable from de-inhibition, both of them reaching similar limiting time courses even at very strong depolarizations.

Furthermore, in the presence of agonist we did not observe any significant change in the time course of tail currents as the depolarization to +80/+120 mV was made longer. By contrast, a change in time course but not in tail current amplitude after longer depolarizations was observed during luteinizing hormone releasing hormone (LHRH) application in sympathetic neurons (Elmslie et al., 1990; Boland and Bean, 1993). According to Boland and Bean, de-inhibition requires the voltage-independent unbinding of the inhibitory molecule and is a distinguishable process from channel opening, which, with large enough depolarizations, can occur with the inhibitory molecule still bound. Our results suggest a new mechanism for Ca^{2+} channel de-inhibition, which differs from that proposed for sympathetic neurons: 1) activation and de-inhibition are indistinguishable processes that require voltage-dependent unbinding of the inhibitory molecule from the channel and 2) the unbinding process must precede channel transition to the open state.

Kinetic models for N-type Ca^{2+} channel inhibition

The voltage-dependent inhibition of N-type Ca^{2+} channels by neurotransmitters is generally attributed to direct binding of activated G proteins to the channel (Swandulla et al., 1991; Lopez and Brown, 1991; Boland and Bean, 1993; Qin et al., 1997; Zamponi and Snutch, 1998). Several models have been proposed to explain how the coupling (channel inhibition), uncoupling (channel de-inhibition), and recoupling (channel re-inhibition) of the two macromolecules occur.

A first model proposed that G protein binding induces a permanently modified gating state of the channels, in slow equilibrium with normal channels (Kasai, 1992; Pollo et al., 1992). However, this model predicts no dependence of the time constants of re-inhibition on agonist concentration, as our results clearly show. According to the models proposed by Bean (1989) and by Elmslie et al. (1990), G protein activation shifts a fraction of the channels to a reluctant state. Brief steps to extreme positive voltages open nearly all of the channels, but most of the channels are in the reluctant-open state. These kinetic schemes have been implemented by Boland and Bean (1993) to obtain concentration-dependent time constants as a consequence of G protein binding and unbinding to the channel. However, according to this model, slow activation becomes slower, not faster, with increasing agonist concentration. This, again, is inconsistent with our data. Furthermore, in both the Elmslie et al. and Boland and Bean models, as the reluctant channels close more rapidly, tail currents are faster in the presence of agonist after brief depolarizations and become slower after long depolarizations. This, again, is inconsistent with our data (Fig. 7). Finally, the Boland and Bean model (1993) predicts that slow activation is faster than slow deactivation; this is the opposite of what we observed (Fig. 5 *B*).

We proposed an alternative model of voltage- and concentration-dependent inhibition, de-inhibition, and re-inhibition of the N-type Ca^{2+} channel caused by agonist action.

In our model we assumed that at rest channels are moved to two inhibited closed states when a certain amount of activated G protein binds to the channel. The inhibited states are supposed to equilibrate with a normally closed state without G protein bound and to which channels are moved by depolarization through voltage-dependent rate constants that are rate limiting for channel activation even at strong membrane depolarizations. Finally, the open state can be reached only from the normally closed state when no G protein is bound any more to the channel.

Indeed, this four-state linear model can reproduce, with good approximation and in a wide voltage range, our most important experimental results. 1) Simulated agonist-modified currents activate after step depolarizations with a time course that is biphasic (Fig. 9, *B* and *C*). 2) Negative to −20 mV the slow time constant of activation τ_s is concentration dependent and increases by decreasing agonist concentration, whereas positive to +20 mV, τ_s values become independent from agonist concentration (Fig. 9 *F*). 3) The simulated time course of re-inhibition is faster than that of de-inhibition in a wide range of depolarizing potentials (Fig. 9 *D*). 4) The simulated rate of re-inhibition at −40 mV increases by decreasing agonist concentration (Fig. 10 *B*). 5) The rate of activation to +80 mV is biphasic and its limiting slow time constant is indistinguishable from the time constant for de-inhibition (Fig. 10 *C*). The fast activating component at +80 mV (not clearly visible in Fig. 10 *C* because of the low time scale) reflects activation of the fraction of unmodulated channels in state C and takes into account the experimentally observed incomplete inhibition even at a saturating agonist concentration. 6) The model accounts for the similar kinetics of the tail currents that follow short or long depolarizations to very positive potentials (inset of Fig. 10 *C*).

Also, our model predicts a high degree of Ca^{2+} channel de-inhibition (38%) after the application of a train of depolarizing pulses mimicking a burst of action potentials (Williams et al., 1997). By contrast, de-inhibition drops to a negligible level by simulating a three times faster re-inhibition time constant, suggesting that only with relatively slow re-inhibition rates could de-inhibition be effectively evoked by physiological stimuli.

Finally, the model predicts that, at ~0 mV, slow activation becomes faster with decreasing agonist concentration. This contrasts with our experimental observations where no significant change in τ_s was measured at 0 mV after changes in agonist concentration. Simulated τ_s is closer to the experimental data, even at 0 mV, when the rate constant d_1 for the unbinding of the first inhibitory molecule from the channel is slowed down by a factor of 0.25 during a change in DPDPE concentration from 1 μM to 10 nM. This, however, would imply a more complicated interaction of the inhibitory molecule with the channel, suggesting, again, a reaction order greater than 2.

Concluding remarks

We would like to believe that a common biochemical and kinetic mechanism is involved in voltage-dependent modulation of calcium channels. Indeed, some of the features reported here agree remarkably well with those reported by others using different cell types and modulators. However, some of our novel experimental results do not agree with other systems; neither can they be simulated by kinetic models such as those suggested by Elmslie et al. (1990) or by Boland and Bean (1993). On the other hand, our model cannot explain some of the features reported by others and not observed in our system, for instance, evidence for reluctant channel openings. At the moment we do not have conclusive explanations for such discrepancies. One possibility could be that the site structure of the N-type channel involved in the binding to the inhibitory molecule differs in distinct cell types, and therefore, these channels could interact differently with the inhibitory molecule. Alternatively, distinct modulators could activate distinct inhibitory molecules that then interact differently with the N-type Ca^{2+} channel. Indeed, Taussig et al., (1992) reported that different transmitters do interact with distinct G proteins to inhibit N-type Ca^{2+} current in NG108-15 cells.

In our model, we assumed that in the two inhibited nonconducting states B_1 and B_2, channels can bind up to two modulatory molecules. If the channel binding sites for the two inhibitory molecules were identical and independent, one would predict rate constants of de-inhibition and re-inhibition as follows: $d_1 = 2d_2$ and $r_2 = 2r_1$. However, such a choice of rate constants did not adequately fit our experimental data. It could be possible that either the two binding sites are not identical or they are not independent. Indeed, the existence on the N-type Ca^{2+} channel α_1 subunit of two distinct binding sites for the $\beta\gamma$ dimer of G proteins has been reported (Qin et al., 1997). Finally, the complex voltage dependence of all four rate constants d_1, d_2, r_1, and r_2 could suggest the interaction of multiple voltage sensors present both on the channel and, eventually, also at the level of the inhibitory molecule (Swandulla et al., 1991).

We thank Dr. K. Dunlap for comments on the manuscript.

This work was supported by INFM-Italy.

REFERENCES

Bean, B. P. 1989. Neurotransmitter inhibition of neuronal calcium currents by changes in channel voltage dependence. *Nature Lond.* 340:153–156.

Boland, L. M., and B. P. Bean. 1993. Bean modulation of N-type calcium channels in bullfrog sympathetic neurons by luteinizing hormone-releasing hormone: kinetics and voltage dependence. *J. Neurosci.* 13: 516–533.

Carabelli, V., M. Lovallo, V. Magnelli, H. Zucker, and E. Carbone. 1996. Voltage-dependent modulation of single N-type Ca^{2+} channel kinetics by receptor agonists in IMR32 cells. *Biophys. J.* 70:2144–2154.

Carbone, E., and D. Swandulla. 1989. Neuronal calcium channels: kinetics, blockade and modulation. *Prog. Biophys. Mol. Biol.* 54:31–58.

Ehrlich, I., and K. S. Elmslie. 1995. Neurotransmitters acting via different G proteins inhibit N-type calcium current by an identical mechanism in rat sympathetic neurons. *J. Neurophysiol.* 74:2251–2257.

Elmslie, K. S., and S. W. Jones. 1994. Concentration dependence of neurotransmitter effects on calcium kinetics in frog sympathetic neurons. *J. Physiol.* 481:35–46.

Elmslie, K. S., W. Zhou, and S. W. Jones. 1990. LHRH and GTP-y-S modify calcium current activation in bullfrog sympathetic neurons. *Neuron.* 5:75–80.

Golard, A., and S. A. Siegelbaum. 1993. Kinetic basis for the voltage-dependent inhibition of N-type calcium current by somatostatin and norepinephrine in chick sympathetic neurons. *J. Neurosci.* 13: 3884–3894.

Grassi, F., and H. D. Lux. 1989. Voltage-dependent GABA-induced modulation of calcium currents in chick sensory neurons. *Neurosci. Lett.* 105:113–119.

Kasai, H. 1992. Voltage- and time-dependent inhibition of neuronal calcium channels by a GTP-binding protein in a mammalian cell line. *J. Physiol. Lond.* 448:189–209.

Kasai, H., and E. Neher. 1992. Dihydropyridine-sensitive and ω-conotoxin-sensitive calcium channels in a mammalian neuroblastoma-glioma cell line. *J. Physiol. Lond.* 448:161–188.

Lopez, H. S., and A. M. Brown. 1991. Correlation between G protein activation and reblocking kinetics of Ca^{2+} channel currents in rat sensory neurons. *Neuron.* 7:1061–1068.

Marchetti, C., E. Carbone, and H. D. Lux. 1986. Effects of dopamine and noradrenaline on Ca^{2+} channels of cultured sensory and sympathetic neurons of chick. *Pflügers Arch.* 406:104–111.

Pollo, A., M. Lovallo, E. Sher, and E. Carbone. 1992. Voltage-dependent noradrenergic modulation of ω-conotoxin-sensitive Ca^{2+} channels in human neuroblastoma IMR32 cells. *Pflügers Arch.* 422:75–83.

Qin, N., D. Platano, R. Olcese, E. Stefani, and L. Birnbaumer. 1997. Direct interaction of G$\beta\gamma$ with a C-terminal G$\beta\gamma$-binding domain of the Ca^{2+} channel α1 subunit is responsible for channel inhibition by G protein-coupled receptors. *Proc. Natl. Acad. Sci. U.S.A.* 94:8866–8871.

Swandulla, D., E. Carbone, and H. D. Lux. 1991. Does calcium channel classification account for neuronal calcium channel diversity? *Trends Neurosci.* 14:46–51.

Taussig, R., S. Sanchez, M. Rifo, A. G. Gilman, and F. Belardetti. 1992. Inhibition of ω-conotoxin-sensitive calcium current by distinct G proteins. *Neuron.* 8:799–809.

Toselli, M., P. Perin, and V. Taglietti. 1995. Muscarine inhibits ω-conotoxin-sensitive calcium channels in a voltage- and time-dependent mode in the human neuroblastoma cell line SH-SY5Y. *J. Neurophysiol.* 74:1730–1741.

Toselli, M., and V. Taglietti. 1994. Muscarinic inhibition of high-voltage-activated calcium channels in excised membranes of rat hippocampal neurons. *Eur. Biophys. J.* 22:391–398.

Toselli, M., P. Tosetti, and V. Taglietti. 1997. μ and δ opioid receptor activation inhibits ω-conotoxin-sensitive calcium channels in a voltage- and time-dependent mode in the human neuroblastoma cell line SH-SY5Y. *Pflügers Arch.* 433:587–596.

Tsunoo, A., M. Yoshii, and T. Narahashi. 1986. Block of calcium channels by enkephalin and somatostatin in neuroblastoma-glioma hybrid NG108–15 cells. *Proc. Natl. Acad. Sci. U.S.A.* 83:9832–9836.

Williams, S., M. Serafin, M. Muhlethaler, and L. Bernheim. 1997. Facilitation of N-type calcium current is dependent on the frequency of action potential-like depolarizations in dissociated cholinergic basal forebrain neurons of the guinea pig. *J. Neurosci.* 17:1625–1632.

Zamponi, G. W., and T. P. Snutch. 1998. Decay of prepulse facilitation of N type calcium channels during G protein inhibition is consistent with binding of a single $G_{\beta\gamma}$ subunit. *Proc. Natl. Acad. Sci. U.S.A.* 95:4035–4039.

Zhou J., M. S. Shapiro, and B. Hille. 1997. Speed of Ca^{2+} channel modulation by neurotransmitters in rat sympathetic neurons. *J. Neurophysiol.* 77:2040–2048.